

Theoretical Investigation of the Role of Choriocapillaris Blood Flow in Treatment of Subfoveal Choroidal Neovascularization Associated With Age-related Macular Degeneration

R. W. FLOWER, C. VON KERCEK, L. ZHU, A. ERNEST, C. EGGLETON,
AND L. D. T. TOPOLESKI

- **PURPOSE:** To investigate the relationship between choriocapillaris blood flow and blood flow through an overlying choroidal neovascularization, as it relates to photocoagulation-induced changes in the choriocapillaris circulation.
- **METHODS:** A theoretical model that simulates the blood flow in the choriocapillaris and choroidal neovascularization of the human eye was developed, based on histologically determined vascular geometry and experimentally measured blood pressure gradients. The choriocapillaris blood pressure and blood flow were examined before and after simulated photocoagulation of various Sattler layer vessels entering the choriocapillaris in the vicinity of the choroidal neovascularization. (The Sattler layer is the inner layer of medium-sized choroidal vessels that includes both arterioles and venules that supply the choriocapillaris.)
- **RESULTS:** The theoretical model showed that both partial and complete occlusion of either Sattler arteriole or venous vessels in the vicinity of the capillary-like vessels connecting a choroidal neovascularization to the underlying choriocapillaris results in significant choroidal neovascularization blood flow reduction. These theoretical results are similar to clinically observed changes induced by laser photocoagulation of feeder vessels. (In this discussion, the term “feeder vessels” refers to those

vessels in an indocyanine green angiogram image that appear to supply blood to a choroidal neovascularization; these vessels appear to be Sattler layer vessels, rather than the histologically demonstrated short, capillary-like vessels that form choriocapillaris–choroidal neovascularization communications.)

- **CONCLUSIONS:** Reduction of choriocapillaris blood flow underlying a choroidal neovascularization may be sufficient to reduce the blood flow rate in the choroidal neovascularization and thereby reduce the associated retinal edema. The results also suggest that reduction of choriocapillaris blood flow may be the common hemodynamic event associated with the successful application of several currently practiced methods of choroidal neovascularization treatment, including feeder vessel photocoagulation, photodynamic therapy, transpupillary thermotherapy, and prophylactic drusen photocoagulation. Ultimately, this model may be useful in determining optimal placement of laser photocoagulation burns to achieve a desirable perturbation in choroidal blood flow distribution and thereby reduce choroidal neovascularization blood flow to the extent necessary to obliterate associated retinal edema. (Am J Ophthalmol 2001; 132:85–93. © 2001 by Elsevier Science Inc. All rights reserved.)

Accepted for publication Jan 8, 2001.

From the Department of Ophthalmology (R.W.F.) and Department of Mechanical Engineering (C.V.K., L.Z., A.E., C.E., L.D.T.T.), University of Maryland, Baltimore, Maryland and the Luesther T. Mertz Retinal Research Lab and the Macular Foundation, Manhattan Eye, Ear, and Throat Hospital (R.W.F.), New York, NY.

Dr Flower is a consultant to Akorn, Inc, US manufacturer of indocyanine green dye.

Reprint requests to R. W. Flower, 11 Dellwood Court, Hunt Valley, MD 21030; e-mail; rflow001@umaryland.edu

PHOTOCOAGULATING THE FEEDER VESSELS SUPPLYING choroidal neovascularization associated with age-related macular degeneration not only can be a successful treatment method,^{1,2} especially for occult choroidal neovascularization, but because of the pretreatment and posttreatment high-speed indocyanine green angiograms the method requires, information about choroidal hemodynamics is being accrued that otherwise probably would not be available. Despite the successes reported in

some cases of feeder vessel photocoagulation, however, there is a predicament associated with defining the nature of feeder vessels themselves: To date no clinically successfully treated feeder vessel has been histologically examined. Therefore, feeder vessels are defined only by their angiographic appearance, and the current gold standard of feeder vessel identification accuracy is a clinically successful outcome after photocoagulation. (In this discussion, the term “feeder vessels” refers to those vessels in an indocyanine green angiogram image that appear to supply blood to a choroidal neovascularization; these vessels appear to be Sattler layer vessels, rather than the histologically demonstrated short, capillary-like vessels that form choriocapillaris/choroidal neovascularization communications.)

An earlier attempt at reconciling the angiographic appearance of feeder vessels with extant histological data about choroidal neovascularization angioarchitecture led to the postulation that feeder vessels are Sattler layer arteriolar vessels that enter the choriocapillaris close to the location of a choroidal neovascularization³; that is, there may not be a direct anatomical connection between a feeder vessel and its associated choroidal neovascularization, but rather only a functional hemodynamic one, resulting from feeder vessel entry into the choriocapillaris near where a short capillary-like vessel penetrates Bruch’s membrane and forms a choriocapillaris/choroidal neovascularization communication. Based on that concept, a simple anthropomorphic model of feeder vessel/choroidal neovascularization blood flow was conceived and demonstrated to account for the clinically observed resolution of retinal edema after feeder vessel photocoagulation, even when only partial feeder vessel closure is achieved.³ However, because the submacular choriocapillaris is a true vascular plexus, fed and drained by multiple interspersed arteries and veins, a much more sophisticated model is needed to describe the changes in choriocapillaris blood flow beneath the choroidal neovascularization after feeder vessel photocoagulation. The goal of this study was to develop such a theoretical model for the human eye choriocapillaris, based on available histologic and hemodynamic data, and to simulate the choriocapillaris blood flow field before and after feeder vessel photocoagulation.

METHODS

AFTER A LITERATURE REVIEW, THE VALUES FOR CHORIOcapillaris and choroidal neovascularization angioarchitectural parameters shown in Table 1 were used to construct the theoretical model of a section of submacular choriocapillaris and a small overlying choroidal neovascularization membrane shown in Figure 1. The choriocapillaris plexus consists of two parallel sheets separated by 7.5 μm , between which 10- μm -diameter columns are placed at regular intervals, leaving 15- μm wide channels in between to simulate the choriocapillaris plexus. Isolated but well

TABLE 1. Submacular Anatomic Parameters

Choriocapillaris	
Capillary cross-sectional diameter	7.5 \times 15 μm^4 , ⁵
Intercapillary space	5 μm^4
Diameter of arteriolar entry to CC	7.6 μm^4
Diameter of venous exit from CC	15 μm^4
Ratio of A/V–CC connections	2:1*
Choroidal neovascular membrane	
Membrane diameter	400 μm^4
Number of penetrating vessels	2 ⁴

CC = choriocapillaris.

*Although the average A/V ratio for eyes is 3:1,⁶ the 2:1 ratio used in this case reflects the ratio that existed in the particular segment of human CC being modeled (see Figure 2).

separated, precapillary arterioles and venules communicate with the choriocapillaris plexus and perfuse it with blood. The cross-sectional dimensions of the arterioles and venules are of the same order as the choriocapillaris thickness, h . The center-to-center spacing between adjacent arterioles and venules is much larger than h . Therefore, the choriocapillaris was modeled as a planar porous medium containing a widely dispersed set of fluid inflows and fluid outflows, simulating the feeding and draining vessels of the Sattler layer. Feeding arteriolar and draining venous vessels consist, respectively, of 7.5- μm diameter and 15- μm diameter tubes entering the choriocapillaris from beneath.

An overlying choroidal neovascularization membrane is modeled as a parallel miniature version of the choriocapillaris, but with smaller dimensions that will result in a significantly higher resistance to fluid flow. The communication between the choroidal neovascularization and the choriocapillaris is by way of two capillary-dimensioned vessels that penetrate Bruch’s membrane (penetrating vessels). In the model, the position of the choroidal neovascularization can be changed in order to achieve various spatial relationships between the penetrating vessels and Sattler layer vessels that feed and drain the choriocapillaris. (The Sattler layer is the inner layer of medium-sized choroidal vessels that includes both arterioles and venules that supply the choriocapillaris.)

This theoretical model became the basis for computer simulation of blood flow distribution in a segment of human subfoveal choriocapillaris approximately 1300 \times 1000 μm (1.3 \times 10⁶ μm^2) in area. The actual placement of multiple Sattler layer vessels to feed and drain blood from the simulated choriocapillaris plexus segment was made according to the histologically determined locations of those vessels in one normal human eye.⁴ Figure 2 (left) shows the anterior aspect of the corrosion cast of a segment of that human submacular choriocapillaris, marked with the actual locations of arteriolar and venous vessels Sattler

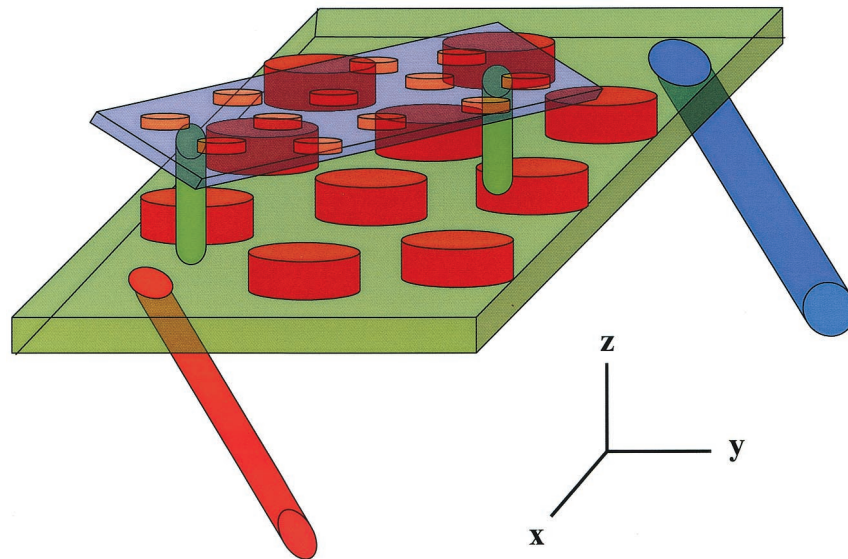


FIGURE 1. Schematic representation of the computer simulated model of the choriocapillaris and an overlying choroidal neovascularization. The choriocapillaris segment is represented by the thin green rectangular box; the red disks within the volume of the box represent the interstitial spaces surrounded by the network of choriocapillaries. One Sattler layer arteriolar (red cylinder) and one venous (blue cylinder) vessel are shown connected to the posterior choriocapillaris. A choroidal neovascularization is represented by the very thin purple rectangular box. The two capillary-like vessels (green cylinders) that penetrate Bruch's membrane (not depicted) and form the choriocapillaris/choroidal neovascularization connection (penetrating vessels) are shown; in the text, these are referred to as penetrating vessels. In the simulation, the position of the penetrating vessels with respect to the Sattler layer vessels was varied.

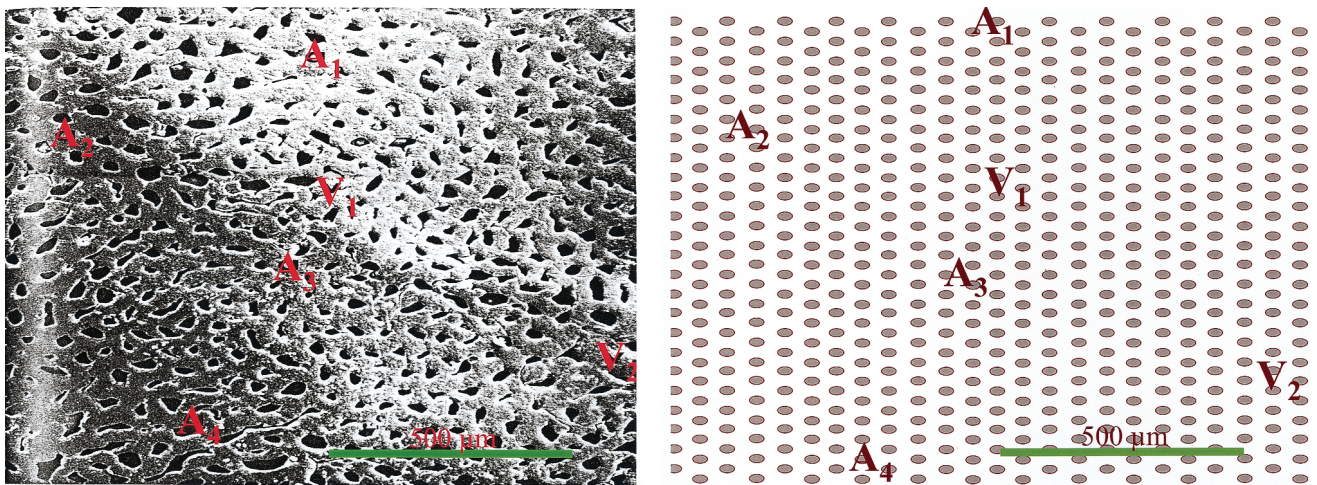


FIGURE 2. (Left) A segment of the anterior aspect of a corrosion cast of the submacular choriocapillaris of a human eye, showing the locations of the arteriolar vessels (A_1 through A_4) and venous vessels (V_1 and V_2) connected to its posterior aspect. (Bottom) The anterior view of the computer-simulated model of the same segment of human choriocapillaris.

layer vessels connected to its posterior aspect. Figure 2 (right) shows the corresponding model layout used in the computer simulation.

In this study, we assumed that the ratio of arterial to venous blood flow rate is 1:2, considering the ratio of the numbers of precapillary arterioles to venules is 2:1. Blood flow rates in the feeding arterioles and venules were then estimated by matching the predicted precap-

illary arteriole and venule pressure difference to experimentally measured data.⁷ The experimentally measured maximum pressure difference between a feeding arteriole and venule was found to be 4.5 mm Hg.⁷ Experimentally measured pressures and pressure differences were applied across the feeding and draining vessels in order to generate maps of blood flow through the computer-simulated model choriocapillaris segment. The

TABLE 2. Submacular Hemodynamic Parameters

Choriocapillaris	
Feeding arteriolar pressure	69 cm H ₂ O ⁷
CC pressure	23.5 cm H ₂ O ⁷
Draining venous pressure	31 cm H ₂ O ⁷
CC pressure drop (A/V)	4.5 mm Hg ⁷
Blood velocity	2 mm/sec ^{8,9}
Apparent blood viscosity	4 × 10 ⁻³ N s/m ² ¹⁰
Choroidal neovascular membrane	
Blood velocity	1 mm/sec

hemodynamic parameters used in the simulation are listed in Table 2.

Because the choriocapillaris blood flow is similar to flow passing a staggered array of circular cylindrical fibers confined between two flat sheets, the theoretical solution for the viscous flow in a channel with periodic cross-bridging fibers by Tsay and Weinbaum¹¹ was employed in the simulation. In this solution that detailed velocity profiles, the drag coefficient f (Figure 9 in reference 12) and the Darcy permeability K_p were presented. For simplification in this study, the choriocapillaris was considered to be a thin porous medium layer, of uniform thickness h , which is much smaller than its lateral dimensions (see Figures 1 and 2B). Applying the choriocapillaris geometry and the tissue fiber volume fraction ($S = 0.14$) measured from Figure 2 (left), f was found to be close to 1.1. Thus the equivalent Darcy permeability could be calculated from equation $K_p = h^2/3f$, and a value of 4.26 μm^2 was obtained.

Let (x,y) be the Cartesian coordinates in the plane of the choriocapillaris (see Figure 1). Let $\vec{V} = (u,v)$ be the planar volume average fluid velocity. The average is taken over a volume that is of order h in size. Darcy's law for the flow in a porous medium is

$$\nabla P = \frac{\mu}{K_p} \vec{V} \quad [1]$$

where K_p is the Darcy permeability, μ is the apparent viscosity of blood including the plasma and cells, and P is the local pressure. It is assumed that the permeability is a constant. Thus, by combining Darcy's law and the continuity equation, it is seen that the pressure field P is a potential resulting from a distribution of sources and sinks. The required pressure field solving this problem is

$$P(x,y) = - \frac{\mu}{K_p} \sum_i q_i \ln \sqrt{(x - x_i)^2 + (y - y_i)^2} \quad [2]$$

where (x_i, y_i) are the coordinates of the feeder vessels measured from Figure 2, and q_i is the line source strengths

defined as the blood flow rates in the feeding vessels divided by the thickness of the choroidal capillary. The blood flow speeds are then readily computed by equations

$$u = \frac{\partial}{\partial x} \sum_i \frac{q_i}{2\pi} \ln \sqrt{(x - x_i)^2 + (y - y_i)^2}$$

$$v = \frac{\partial}{\partial y} \sum_i \frac{q_i}{2\pi} \ln \sqrt{(x - x_i)^2 + (y - y_i)^2} \quad [3]$$

Equations (2) and (3) enable us to predict the blood speed and pressure fields in the choriocapillaris resulting from a particular distribution of blood flow in the feeding arterioles and venules.

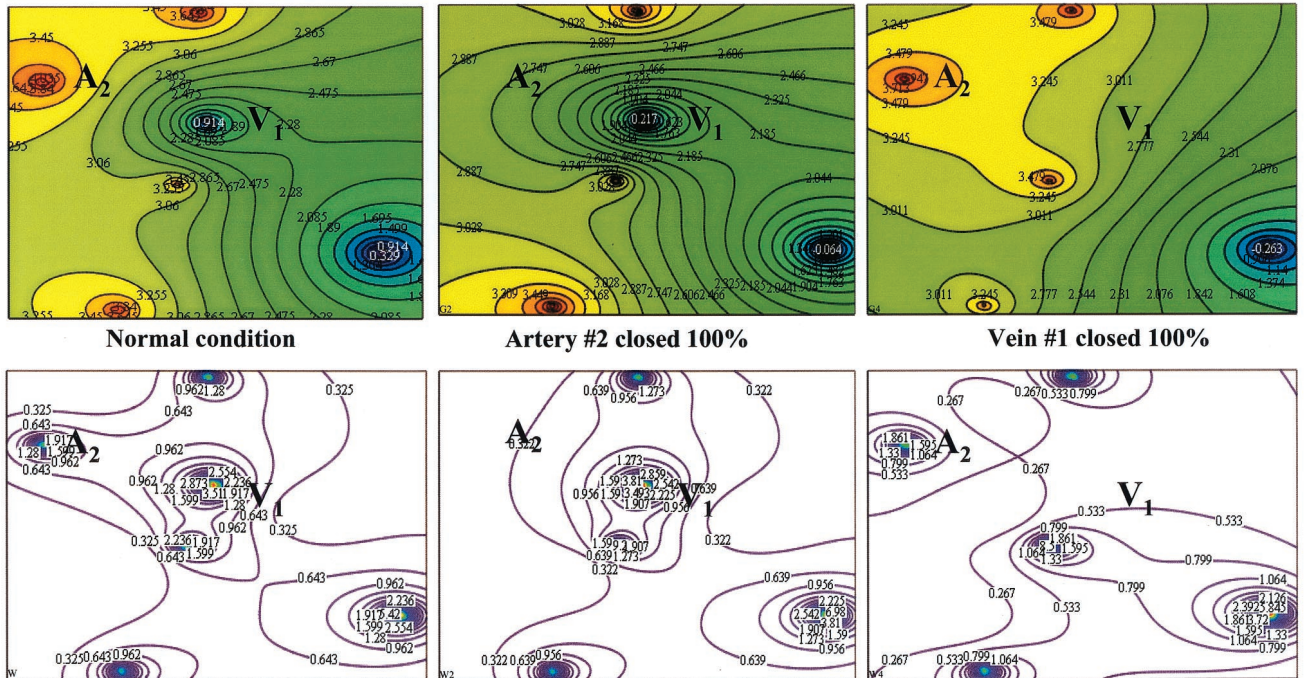
The blood pressure and blood speed fields before and after photocoagulation of the various Sattler layer vessels in communication with the model choriocapillaris segment were then simulated to evaluate the effects of indirect laser treatment on choriocapillaris blood flow patterns. Additionally, the effects on blood flow through overlying choroidal neovascularizations were simulated. (For purposes of the simulation, it was assumed that blood flow through a choroidal neovascularization is small relative to that through the choriocapillaris and thus has little effect on the nominal choriocapillaris flow pattern and pressure gradients generated by the feeding arterioles and venules.) The results obtained from the computer simulations were then compared with clinically observed changes induced by various laser photocoagulation treatments of choroidal neovascularization.

RESULTS

THE EFFECTS ON CHORIOCAPILLARIS BLOOD FLOW OF PARTIALLY or completely closing a Sattler layer vessel entering the choriocapillaris plexus (that is, feeder vessel) were demonstrated by comparing the choriocapillaris blood pressure and blood speed fields before and after simulated laser photocoagulation. The blood flow rate in an overlying choroidal neovascularization could then be simulated according to the local pressure difference between its points of communication with the choriocapillaris (that is, between its penetrating vessels; see Figure 1).

Figure 3 shows the normal isobar and iso-blood-speed distributions in the computer-simulated segment of choriocapillaris from Figure 2; it also shows how those distributions are altered when a single feeding or draining vessel is occluded. The pressure was normalized to be zero at the draining venule, and the blood flow rates in the communicating Sattler layer arterioles and venules were adjusted so that the maximum pressure difference between any arteriole and venule was approximately 4.5 mm Hg. The blood speed at the midpoint between any feeder arteriole and venule was found to be approximately 1 mm per

CC Blood Pressure Field (mm Hg)



CC Blood Speed Field (mm/sec)

FIGURE 3. Isogramic maps of the blood pressure and blood speed fields of the choriocapillaris segment shown in Figure 2 under normal and simulated vascular photocoagulation conditions. The isogramic lines in the left-hand two frames identify locations of constant pressure (upper frame) and flow (lower frame) throughout the choriocapillaris (CC) segment under normal conditions. The pattern of these lines changes, as shown in the other pairs of frames, when either the underlying Sattler layer arteries (middle frames) or veins (right frames) are occluded. The particular vessels occluded in these examples are arteriole A_1 and venule V_1 identified in Figure 2.

second, which is consistent with the measured data from the literature.^{8,9}

When blood flow rate in arteriole 2 was decreased by 50% and 100%, corresponding decreases of 30% and 70% occurred in the local pressure gradient in the vicinity of arteriole 2 and venule 1 (Figure 2). On the other hand, the results show that the simulated photocoagulation occlusion has only a minor effect on the pressure field far away from the targeted feeder vessel. Similarly, up to 50% and 80% decreases in the local pressure gradient were induced, respectively, by partial (50%) and complete closures of venule 1. The result that 50% occlusion of a feeder vessel has a significant effect on the pressure field, albeit not as dramatic as a complete occlusion, is interesting. However, it was surprising to find that same magnitude decrease in the local choriocapillaris pressure field results from closing either an arteriole or a venule.

A significant reduction in the local choriocapillaris

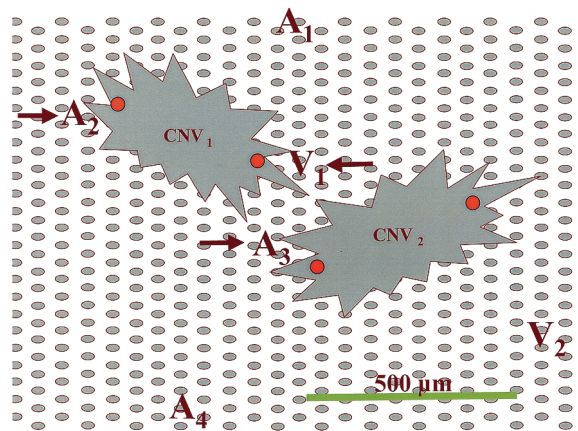


FIGURE 4. The anterior view of the computer-simulated choriocapillaris segment shown in Figure 2, illustrating two locations of a simulated overlying choroidal neovascularizations. Arrows indicate specific arteriolar and venous vessels arising from the Sattler layer on which simulated photocoagulations were performed. CNV = choroidal neovascular membrane.

pressure probably results in significant changes in the blood flow through an overlying choroidal neovascularization, because the driving force for choroidal neovascular blood flow is the pressure difference between the choroidal neovascularization's penetrating vessels. Clinical observations indicate that partial, as well as complete, photocoagulation of the (presumed Sattler layer) feeder vessel adjacent to a choroidal neovascularization's penetrating vessel(s) is an effective means of decreasing the blood flow in the choroidal neovascularization (BM Glaser, RP Murphy, G Staurengi, personal communications, 1999). Therefore, to evaluate further the blood flow through a choroidal neovascularization before and after feeder vessel laser photocoagulation, we simulated blood flow through a choroidal neovascularization situated in two different locations, as indicated in Figure 4. The first location, choroidal neovascularization 1, was between arteriole 2 and venule 1, while the second, choroidal neovascularization 2, was between arteriole 3 and a point in the venous pressure field equidistant from venules 1 and 2. For simplicity, the choroidal neovascularizations were approximated as a simple pipe entering and exiting the choriocapillaris from above. The flow resistance through the choroidal neovascularization was estimated by the Hagen-Poiseuille equation for a rigid pipe:

$$Q = \Delta P / R_{CNV}$$

$$\text{where } R_{CNV} = (8L\mu) / (\pi r_{CNV}^4) \text{ and } Q = \pi r_{CNV}^2 \text{ } [4]$$

A rough estimate of the choroidal neovascular luminal radius (r_{CNV}) was $5.5 \mu\text{m}$, and the length of the choroidal neovascularization (L) was approximately $400 \mu\text{m}$; these dimensions are roughly compatible with the dimensions of the choroid capillaries. The flow velocities through the choroidal neovascularization for these two locations were estimated by equation 4, before and after simulated laser photocoagulation of the feeding vessels near the choroidal neovascularization's penetrating vessels. The results are graphed in Figures 5 and 6. The normal velocities calculated from this simple equation are of the same order as that in the choriocapillaris, which is consistent with the clinical observation that choroidal neovascular indocyanine green dye filling ranges from about the same to about one half that of the choriocapillaris. Photocoagulation of arteriole 2 and of venule 1 resulted in significant reduction of choroidal neovascular membrane 1 blood flow, with similar results in choroidal neovascularization 2 when arteriole 3 was photocoagulated. On the other hand, even the complete closure of venules 1 or 2 produced less than a 30% decrease in blood velocity through choroidal neovascular membrane 2.

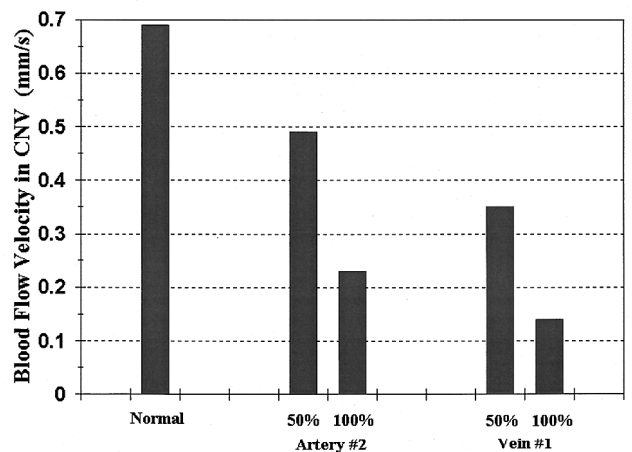


FIGURE 5. Velocity of blood through the choroidal neovascularization (CNV) in position 1 in Figure 4, under normal conditions and after simulated photocoagulation of an artery and vein feeding the underlying choriocapillaris. Changes in the blood pressure and blood flow distributions through the area of choriocapillaris shown in Figure 2, resulting from simulated occlusion of a Sattler layer arteriole (A_2) and venule (V_1).

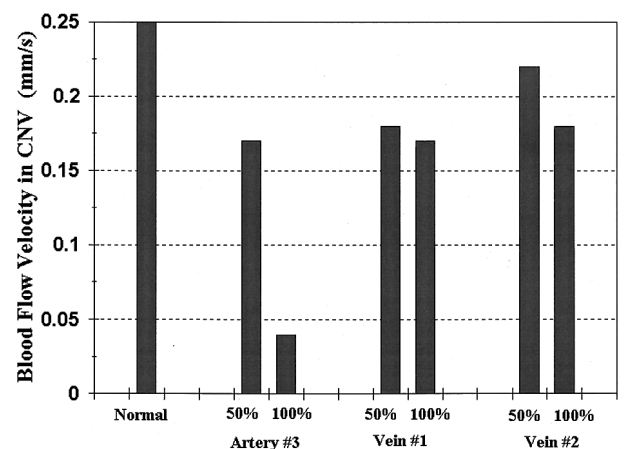


FIGURE 6. Velocity of blood through the choroidal neovascularization (CNV) in position 2 in Figure 4, under normal conditions and after simulated photocoagulation of an artery and vein feeding the underlying choriocapillaris.

DISCUSSION

AN IMPORTANT CONCEPT OF THE CHOROIDAL VASCULAR model on which the computer simulations were based is that feeder vessels are Sattler layer arteriolar vessels entering the choriocapillaris close to the location of a choroidal neovascularization.³ There appears to be additional clinical evidence supporting that concept: A commonly observed characteristic of successfully treated feeder vessels was their "beaded" appearance in pretreatment indocyanine green angiograms (RP Murphy, symposium presentation, Chicago, June 3, 2000); an example of that

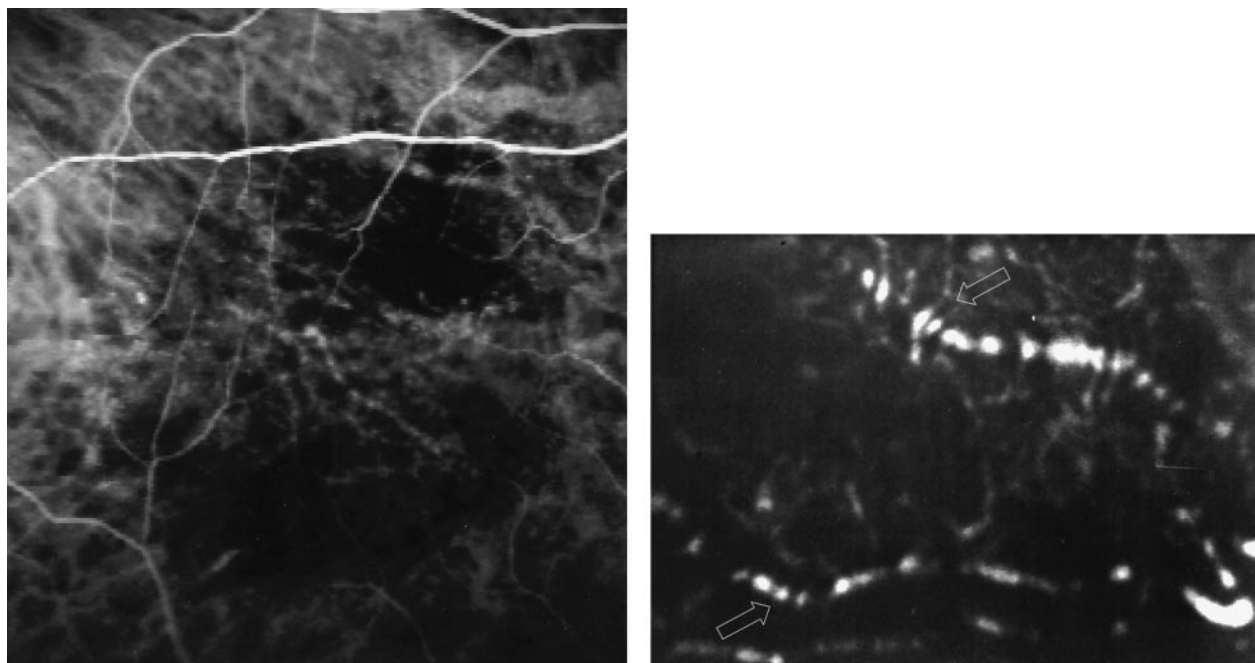


FIGURE 7. (Left) Image from a human indocyanine green angiogram showing the “beaded” appearance of a successfully treated choroidal neovascularization feeder vessel. The feeder vessel originates in the center of the field of view and extends infranasally toward the choroidal neovascularization, which lies in the slightly hypofluorescent inferior area. (Right) Image from a rhesus monkey indocyanine green angiogram, made after carotid arterial injection of dye. Because of the improved dye wave front definition produced from arterial dye injection, temporal differences in filling of various layers of choroidal vessels are enhanced. When crossed by small non-dye-filled vessels, the crossings result in dark segments along the feeder vessel (the lower arrow); when crossed by small dye-filled vessels, the crossings result in hyperfluorescence, resulting from additivity of fluorescence from the overlapping vessels (the upper arrow). The presence of small vessels between the feeder vessel and the choriocapillaris fixes the feeder vessel location well below the choriocapillaris, consistent with the notion that feeder vessels do arise from the Sattler layer.

appearance is shown in Figure 7 (left). The most likely explanation for the beaded appearance is that the dye-filled feeder vessel is crossed throughout its length by smaller choroidal vessels. This same phenomenon is more pronounced in high-speed indocyanine green angiograms of rhesus monkey eyes after carotid arterial dye injection, as demonstrated in Figure 7 (right), wherein carotid dye injection improves dye wave front definition, enhancing observation of the temporal filling differences between various layers of choroidal vessels. When crossed by small non-dye-filled vessels, the crossings result in dark segments along the feeder vessel; when crossed by small dye-filled vessels, the crossings result in hyperfluorescence, because of additivity of fluorescence from the overlapping vessels. The presence of small vessels between the feeder vessel and the choriocapillaris fixes the feeder vessel location well below the choriocapillaris, consistent with the notion that feeder vessels are in the Sattler layer.

The computer-simulated choriocapillaris and choroidal neovascular blood flows generated during this investigation assumed that the vessel walls of the choroidal vascular model were rigid and that blood pressure and blood flow rates through it were steady state. A more sophisticated model would incorporate flexible vessel walls and pulsatile blood

flow, but not enough data exist currently to make implementation of such refinements realistic. Nevertheless, results derived from the simulations do support the concepts raised earlier, namely that (1) the vessels termed choroidal neovascularization feeder vessels lie in the Sattler layer and enter the choriocapillaris in close proximity to the penetrating vessels that form the choriocapillaris/choroidal neovascularization communication, and (2) even partial occlusion of a feeder vessel may be sufficient to effectively stop choroidal neovascularization blood flow.³ It is intuitive, however, that with such refinements to the model system, blood flow resistance of the modeled choroidal neovascularization would be more sensitive to the local pressure gradient; that is, if the diameter of the pipe representing the choroidal neovascularization reduced in response to decrease in the pressure difference or blood flow rate, smaller velocities (blood flow rates) would result than those predicted in Figures 5 and 6. Additionally, the choroidal neovascularization probably would require a “threshold” pressure gradient to be open. This augurs more strongly that incomplete laser photocoagulation of an associated feeder vessel could result in obliteration of choroidal neovascular blood flow even if the pressure gradient across it were not reduced completely to zero, permitting retention of underlying choriocapillaris circulation.

The present model predicts that even 50% closure of a blood vessel entering the posterior aspect of the choriocapillaris in the vicinity of a choroidal neovascularization's penetrating vessels can be effective in reducing or possibly stopping choroidal neovascular blood flow, regardless of whether that vessel is a feeding arteriole or a draining venule. In other words, the important hemodynamic event with respect to reducing or stopping choroidal neovascular blood flow is significant reduction of the blood pressure and, hence, blood flow as well, in the local underlying choriocapillaris. Thus the predictions of the present computer-simulated model support the novel approach to choroidal neovascularization management made previously, namely that (1) rather than total obliteration of a choroidal neovascularization (which frequently results in recurrence), the end point of laser photocoagulation treatment can be reduction of choroidal neovascular blood flow to the extent that undesirable manifestations of the choroidal neovascularization, most notably retinal edema, are halted or reversed; and (2) that choroidal neovascular blood flow reduction can be mediated by reduction of blood flow through the underlying choriocapillaris.³

There are two important implications to that novel approach, one related to feeder-vessel treatment and the other related to the mechanics of successful choroidal neovascular treatments in general. Regarding feeder-vessel photocoagulation treatment of choroidal neovascularization, the selection criterion for targeted "feeder vessels" might be extended to include venous as well as arteriolar vessels entering the posterior choriocapillaris in the vicinity of a choroidal neovascular membrane. If indeed reduction of the underlying choriocapillaris blood flow is the important treatment goal, then depending on the orientation of the choroidal neovascular membrane's penetrating vessels with respect to the field of vessels feeding and draining the choriocapillaris, targeting veins or veins in conjunction with arteries may yield the best results. After all, the ramifications of occluding a venous drainage channel to a true vascular plexus, like the posterior pole choriocapillaris, is not the same as occlusion of the drainage vein of a true end-arteriolar vascular complex. In the former case, blood is diverted to adjacent venous channels, without excessive increase in capillary transmural pressure, whereas in the latter case, venous occlusion likely results in blood flow stasis and elevation of capillary transmural pressure to a level near that across the feeding arterial vessel wall.

Because the predicted relationship between choriocapillaris and choroidal neovascular blood flows actually is independent of the specific means by which choriocapillaris blood flow is reduced, the second implication of the results is that reduction of choriocapillaris blood flow underlying a choroidal neovascularization may be a component mechanism common to successful choroidal neovascularization photocoagulation treatments, including photodynamic therapy, transpupillary thermal therapy,

and drusen photocoagulation. It is well established that post-photodynamic therapy angiograms routinely show evidence of reduced choriocapillaris fluorescence,¹² and that appears also to be the case after transpupillary thermal therapy.¹³ In the case of transpupillary thermal therapy, reduced choriocapillaris blood flow may be the result of increased resistance to plexus blood flow resulting from heat-induced interstitial tissue swelling and concomitant reduction of choriocapillaris luminal space. Angiographic data specifically related to submacular blood flow after photocoagulation destruction of macular drusen have not been presented anywhere; however, it has been demonstrated that choriocapillaris obliteration occurs with application of moderate to heavy laser burns and that loss of choriocapillaries can add significant resistance to blood flow through the choriocapillaris plexus.¹⁴

If reduced choriocapillaris blood flow is a component mechanism of successful choroidal neovascular treatment, regardless of the photocoagulation modality used, then feeder-vessel photocoagulation arguably might be viewed as the most effective method. The difference between feeder-vessel photocoagulation and the other methods is analogous to removing a weed from a lawn by pulling out its roots (feeder vessel) versus just cutting off the weed's leaves. It can be argued that feeder-vessel photocoagulation is the most precise of the various methods in terms of manipulating choriocapillaris blood flow, and it minimizes the area of tissue/laser interaction. Moreover, because blood flow through a particular choriocapillaris area apparently can be manipulated by modulation of adjacent venous or as arteriolar vessels connected to the plexus' anterior side, it may be that the most precise manipulation of choriocapillaris blood flow and hence treatment of choroidal neovascularization, will be by controlled, partial photocoagulation of carefully selected combinations of arterioles and venules in the Sattler layer.

REFERENCES

1. Shariga F, Ojima Y, Matsuo T, Takasu I, Matsuo N. Feeder vessel photocoagulation of subfoveal choroidal neovascularization secondary to age-related macular degeneration. *Ophthalmology* 1998;105:662-669.
2. Staurengi G, Orzalesi N, La Capria A, Aschero M. Laser treatment of feeder vessels in subfoveal choroidal neovascular membranes: a revisit using dynamic indocyanine green angiography. *Ophthalmology* 1998;105:2297-2305.
3. Flower RW. Experimental studies of indocyanine green dye-enhanced photocoagulation of choroidal neovascularization feeder vessels. *Am J Ophthalmol* 2000;129:501-512.
4. Fryczkowski AW, Sherman MD. Scanning electron microscopy of human ocular vascular casts: the submacular choriocapillaris. *Acta Anat* 1988;132:265-269.

5. Spraul CW, Lang GE, Grossniklaus HE. Morphometric analysis of the choroid, Bruch's membrane, and retinal pigment epithelium in eyes with age-related macular degeneration. *Invest Ophthalmol Vis Sci* 1996;37:2724–2735.
6. Fryczkowski AW, Sherman MD, Walker J. Observations on the lobular organization of the human choriocapillaris. *Int Ophthalmol* 1991;15:109–120.
7. Maepea O. Pressures in the anterior ciliary arteries, choroidal veins and choriocapillaris. *Exp Eye Res* 1992;54:731–736.
8. Flower RW. Variability in choriocapillaris blood flow distribution. *Invest Ophthalmol Vis Sci* 1995;36:1247–1258.
9. Koyama T. Experimental studies of the microcirculation, III: High speed cinematographic analysis of choriocapillary blood flow. *Acta Soc Ophthalmol Jpn* 1981;85:1–6.
10. Fung YC. *Biomechanics: mechanical properties of living tissues*, 2nd edition. New York: Springer-Verlag, 1993.
11. Tsay R-Y, Weinbaum S. Viscous flow in a channel with periodic cross-bridging fibres: exact solutions and Brinkman approximation. *J Fluid Mech* 1991;226:125–148.
12. Flower RW, Snyder WA. Expanded hypothesis on the mechanism of photodynamic therapy action on choroidal neovascularization. *Retina* 1999;19:365–369.
13. Reichel E, Berrocal AM, Ip M, et al. Transpupillary thermotherapy (TTT) of occult subfoveal choroidal neovascularization in patients with age-related macular degeneration. *Ophthalmology* 1999;106:1908–1914.
14. Flower RW. Extraction of choriocapillaris hemodynamic data from ICG fluorescence angiograms. *Invest Ophthalmol Vis Sci* 1993;34:2720–2729.

The full-text of AJO is now available online at www.ajo.com. Authors Interactive®, currently available in limited form, is undergoing an upgrade.